Structural evolution due to Zn and Te adsorption on As-exposed Si(211): density functional calculation

2009 J. Phys.: Condens. Matter 21 375502

(http://iopscience.iop.org/0953-8984/21/37/375502)

J. Phys.: Condens. Matter **21** (2009) 375502 (7pp) doi:10.1088/0953-8984/21/37/375502

Structural evolution due to Zn and Te adsorption on As-exposed Si(211): density functional calculation

Bikash C Gupta[1], **Shyamal Konar**[1], **C H Grein**[2] **and S Sivananthan**[2]

[1] Department of Physics, Visva-Bharati, Santiniketan 731235, India
[2] Department of Physics, University of Illinois at Chicago, 845 W Taylor Street, Chicago, IL 60607-7059, USA

Received 6 June 2009, in final form 4 August 2009
Published 21 August 2009
Online at stacks.iop.org/JPhysCM/21/375502

Abstract
Systematic theoretical investigations are carried out under the density functional formalism in an effort to understand the initial structural evolution due to the adsorption of ZnTe on As-exposed Si(211). Our calculations indicate that after the adsorption of Zn and Te on the As-exposed Si(211), the stable atomic structure qualitatively follows the ideal atomic structure of Si(211) with alteration of various bond lengths. Since the basic symmetry of the Si(211) is preserved after the adsorption of ZnTe, the deposition of ZnTe on the As terminated Si(211) prior to the deposition of CdTe and HgCdTe is useful for obtaining an ultimate quality layer of HgCdTe on Si(211). Some of our results are compared with the available experimental results, and they are found to agree with each other qualitatively.

(Some figures in this article are in colour only in the electronic version)

1. Introduction

As silicon substrates are often used for the development of technological devices, Si surfaces continue to be a subject of intense theoretical and experimental studies. Extensive investigations have been done on the low index Si surfaces, for example, Si(001) and Si(111) [1, 2]. Most of the theoretical investigations have been confined to low index surfaces due to the 'simplicity' of the surface. However, the high index surfaces such as Si(211), Si(311), Si(331), Si(557), and Si(553), have attracted great attention recently [3–19]. High index surfaces are proven to play a technologically important role as substrates for the fabrication of large wavelength infrared detectors [6–9] and as substrates for the formation of metallic nanowires [12–14].

Many of the high index Si surfaces are complicated in structure due to the existence of terraces and steps. The surface of interest here is Si(211) which can be looked upon as a stepped arrangement of narrow (111) terraces. A three-dimensional view of a small portion of the ideal Si(211) surface is shown in figure 1. The atoms marked T (called the terrace atoms) on the terrace are three-fold coordinated and thus have one dangling bond each; those on the step edge, marked E (called the edge atoms) are two-fold coordinated and have two dangling bonds each. Atoms in the second layer and closest to the edge atoms are denoted as Tr (called the trench atoms) and have one dangling bond each. The Si(211) surface consists of two-atom wide terraces between terrace and edge atoms along

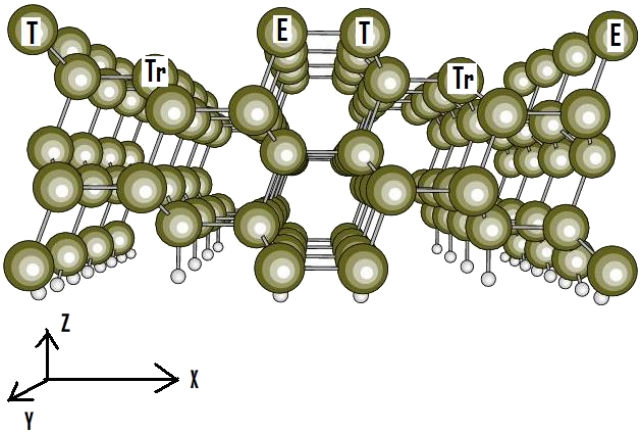

Figure 1. Atoms in perspective form the ideal Si(211) 2×8 supercell. The bottom layer Si atoms are passivated by hydrogen atoms (small circles). Surface terrace, trench and edge atoms are denoted as T, Tr and E, respectively. The X, Y and Z directions correspond to $[\bar{1}11]$, $[01\bar{1}]$ and [211], respectively.

the [$\bar{1}$11] direction. Two consecutive terraces are separated by steps and are 9.4 Å apart in the [$\bar{1}$11] direction, while they extend infinitely along [01$\bar{1}$].

The reconstruction of Si(211) has been studied by various groups earlier [16–19]. However, a recent study by Baski *et al* [10, 11] was conclusive, the authors showed in their STM images that the clean Si(211) is unstable and it consists of nanofacets with (111) and (337) orientations. As there is evidence [12] that the (211) orientation is regained due to metal adsorption on Si(211), the bulk terminated Si(211) surface was used to study the As adsorption on Si(211) [24].

It has been claimed in recent experiments [9, 20] that the epitaxial growth of II–IV materials on an As terminated Si surface gives a better quality film compared to that on a bare Si surface. For example, a high quality interface and better ZnS films were obtained [20] with As-exposed Si(001). Good quality CdTe layers have been grown on the Si(211) surface for subsequent growth of HgCdTe [6–8]. In particular, our motivation for studying Si(211) is due to emerging experimental interest in epitaxial growth of HgCdTe after a successive growth of ZnTe and CdTe on the As-exposed surfaces aimed at developing large area focal plane arrays for the fabrication of detectors [9, 21]. Here we note that an earlier study [19], to understand the interaction of As on Si(211), revealed important results, however, it was incomplete. There were speculations [22] based on the analysis by Bringans [23] that As atoms may replace surface Si atoms instead of being adsorbed on Si(211). Another comprehensive study [24] presented the stable atomic configuration of As on the Si(211) surface and concluded that 66% of surface Si atoms are replaced by As atoms. This result qualitatively agrees with the recent experimental result for As coverage on Si(211) [25, 26]. However, we are yet to understand the surface modification and the atomic structure when ZnTe is adsorbed on the As-exposed Si(211) prior to the deposition of CdTe and HgCdTe. We therefore, carry out extensive electronic structure calculations to understand the atomic structure due to the adsorption of Te and Zn on the As terminated Si(211).

Recently [27], Auger-electron spectroscopy was used to determine the Te coverage on an As-exposed Si(211) surface and it was found that only approximately 20–30% of a monolayer (ML) of Te is bonded to the Si(211) surface. Here 1 ML coverage corresponds to one atom per surface Si atom. There was a theoretical attempt to find the Te coverage on the As-exposed Si(211) and the results were incomplete [24]. Later, another experimental study [26] based on the x-ray photoelectron spectroscopy showed that the Te coverage on the As-exposed Si(211) is around 27% of 1 ML coverage. These experimental results also encourage us to carry out energetics calculations for the Te adsorption on the As-exposed Si(211). Our total energy calculations here reveal that Te coverage on the As-exposed Si(211) is preferably 33% of 1 ML which qualitatively agrees with the experimental result [26, 27]. In addition, we conclude that the atomic structure of Si(211) after the adsorption Te and Zn follows qualitatively the ideal Si(211) structure and therefore, the deposition of ZnTe is suggestive prior to the deposition of CdTe and HgCdTe.

The paper is organized as follows. In section 2 we present the parameters used in the pseudopotential density functional calculations. The results and discussions are presented in section 3. Finally, in section 4, we summarize our principal results.

2. Method

Total energy minimization calculations are carried out within the density functional theory (DFT) in conjunction with the pseudopotential approximation. The Si(211) surface is represented in a repeated slab geometry. Each slab contains seven Si(211) layers with a vacuum region of 15 Å. Within the 1×2 supercell, each layer contains four Si atoms: two along [$\bar{1}$11] and two along [01$\bar{1}$]. The Si atoms in the bottom layer have their dangling bonds and they are saturated by H atoms (see figure 1). Since the edge atoms have two dangling bonds each, the trench atoms have one dangling bond each and the terrace atoms have one dangling bond each, we require 8 H atoms to saturate all the dangling bonds at the bottom of the slab within the 1×2 supercell. The top five Si layers are allowed to relax for geometry optimization while the two lower-most Si layers and the H atoms passivating the Si atoms at the bottom of the slab are held fixed to simulate the bulk-like termination. The wavefunctions are expanded in a plane wave basis set with a cutoff energy $|\vec{k}+\vec{G}|^2 \leqslant 350$ eV. The Brillouin zone (BZ) integration is performed within a Monkhorst–Pack (MP) [28] scheme using 12 inequivalent k-points. It has been established earlier [19] that this energy cutoff and k-points give sufficiently converged values for the binding energies. Ionic potentials are represented by Vanderbilt-type ultra-soft pseudopotentials [29] and results are obtained using the generalized gradient approximation (GGA) [30] for the exchange–correlation potential. A preconditioned conjugate gradient is used for wavefunction optimization and a conjugate gradient for ionic relaxations. The convergence criterion for energy is taken to be 10^{-5} eV and the systems are relaxed until the forces are below 0.005 eV Å^{-1}. The Z axis is taken perpendicular to the Si(211) surface, while X and Y axis are along [$\bar{1}$11] and [01$\bar{1}$], respectively. The VASP code [31] is used for our calculations.

3. Results and discussions

3.1. Arsenic passivated Si(211) surface

Earlier theoretical calculations [24] showed that 66% of surface Si atoms of Si(211) are replaced by As atoms, i.e., the As coverage on the Si(211) surface is 2/3 of a monolayer (ML). Here one ML corresponds to one atom per surface Si atom of the Si(211) surface, for example, adsorption of three atoms in 1×1 supercell correspond to 1 ML coverage. This theoretical prediction of 2/3 ML coverage on the Si(211) surface agrees with the experimental findings. However, the detailed microscopic analysis of the atomic structure was not presented earlier. The atomic structure of the As-exposed Si(211) surface is reproduced and shown in figure 2. All the terrace and trench Si atoms of Si(211) surface are replaced by As atoms. To have an idea about the nature of bonding of As atoms with neighboring Si atoms, we plot the total charge

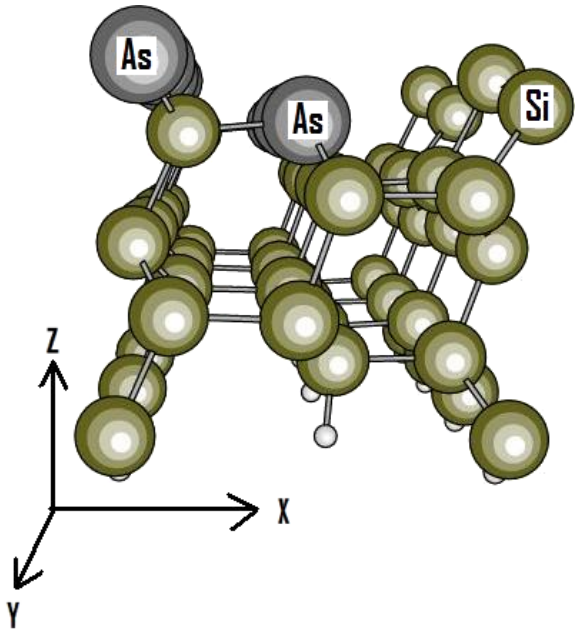

Figure 2. Atomic structure of As-exposed Si(211) within the 1 × 4 supercell. The terrace and trench Si atoms are replaced by As atoms. X, Y and Z directions correspond to $[\bar{1}11]$, $[01\bar{1}]$ and [211], respectively.

density along a line joining an As atom and its nearest Si atom (see figure 3). Figure 3 clearly shows an accumulation of charge at the center of the As–Si bond and therefore, the As atoms bond with the neighboring Si atoms covalently. The Si–As bond lengths are ∼2.39 Å, this implies that the As atoms make a strong bond with the surface Si atoms. Also notice that the edge Si atoms form buckled dimers with a Si–Si bond length of 2.3 Å and alternate As atoms at terrace and trench sites have equal height. Therefore, the As-passivated Si(211) surface reconstructs into a 1 × 2 pattern.

3.2. Te and Zn adsorption on As-passivated Si(211) surface: the first approach

Here we consider the adsorption of Te and Zn on the As-passivated Si(211):1 × 2 surface. As the Si(211) surface reconstructs into the 1 × 2 pattern, we consider the 1 × 2 supercell for the adsorption of Te and Zn. Following the experimental procedure, we first consider the adsorption of Te atoms on the As-exposed Si(211):1 × 2 surface within the 1 × 2 supercell. There are various symmetric sites for Te adsorption. To understand the most favorable site we calculate the binding energy (BE) for the adsorbed atom and it is defined as follows.

$$\mathrm{BE} = E_t[\mathrm{Sub} + \mathrm{AA}] - E_t[\mathrm{Sub}] - E_a[\mathrm{Sub}] - E_a[\mathrm{AA}] \quad (1)$$

where, $E_t[\mathrm{Sub} + \mathrm{AA}]$, $E_t[\mathrm{Sub}]$, $E_a[\mathrm{Sub}]$ and $E_a[\mathrm{AA}]$ correspond to the total energy of the substrate with one atom adsorbed, the total energy of the substrate, the atomic energy of the substrate and the atomic energy of the adsorbed atom, respectively. The systematic calculations reveal that at 1/6 ML Te coverage, the Te atom (within the 1 × 2 supercell) binds strongly with the edge Si atoms with a binding energy of

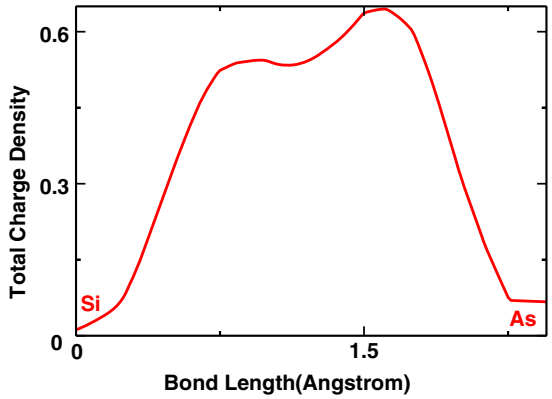

Figure 3. The total charge density along a line of As–Si bond of the As-passivated Si(211) surface.

∼4.47 eV and the Te–Si bond lengths turn out to be ∼2.6 Å. The total charge density plot in figure 4(a) also clearly shows the strong bonding of the Te atom with the neighboring edge Si atoms at 1/6 ML coverage of Te. To understand the nature of the Te–Si bond more clearly, we have plotted the charge density (see figure 4(b)) along a Te–Si bond. It shows that the Te–Si bond is covalent in nature. However, at 1/6 ML coverage of Te, the surface reconstruction pattern remains 1 × 2. The energy gain (ΔE) due to adsorption of a single Te atom within the 1 × 2 supercell of As-exposed Si(211) is obtained by using $\Delta E = (\mathrm{BE} - |\mu_{\mathrm{Te}}|)$, where μ_{Te} is the chemical potential of Te. Considering the upper bound of the μ_{Te}, i.e., the bulk chemical potential of Te, $\mu_{\mathrm{Te}}^{\mathrm{Bulk}} = -3.16$ eV, the maximum energy gain per Te atom at 1/6 ML Te coverage is $\Delta E_{\mathrm{max}} \sim 1.3$ eV. Thus, the adsorption of 1/6 ML Te on the As-exposed Si(211) surface is energetically permitted.

The Te coverage is now increased to 1/3 ML by adsorbing one more Te atom within the 1 × 2 supercell. In the presence of the first Te atom, the second Te atom prefers to bind again with the edge Si atoms and the binding energy of the second Te atom is ∼4.48 eV. At 1/3 ML coverage of Te, the edge Si dimers are broken and hence, the surface reconstruction is almost lifted and all the dangling bonds of edge Si atoms are saturated. All the Te–Si bond lengths optimizes to 2.54 Å and therefore, at 1/3 ML coverage of Te, the Te–Si bonds become stronger when compared with that at 1/6 ML coverage of Te. The favorable atomic structure of the 1/3 ML Te covered, As-passivated Si(211) is shown in figure 5. This clearly indicates that the Si(211) mostly regains its ideal structure. Note that the maximum energy gain due to the adsorption of the second Te atom in the presence of the first Te atom within the 1 × 2 supercell of the As-exposed Si(211) surface is ∼1.3 eV. Thus the adsorption of 1/3 ML Te is energetically allowed on the As-exposed Si(211) surface.

The Te coverage is further increased to 1/2 ML by placing another Te atom in the presence of two Te atoms within the 1 × 2 supercell. We find that the third Te atom prefers to be on top of a trench As atom and the binding energy of the third Te atom drastically reduces to 1.9 eV. In this case, the BE of the third Te atom is less than the $|\mu_{\mathrm{Te}}^{\mathrm{Bulk}}|$ by 1.26 eV and therefore, we need to supply at least 1.26 eV for binding the

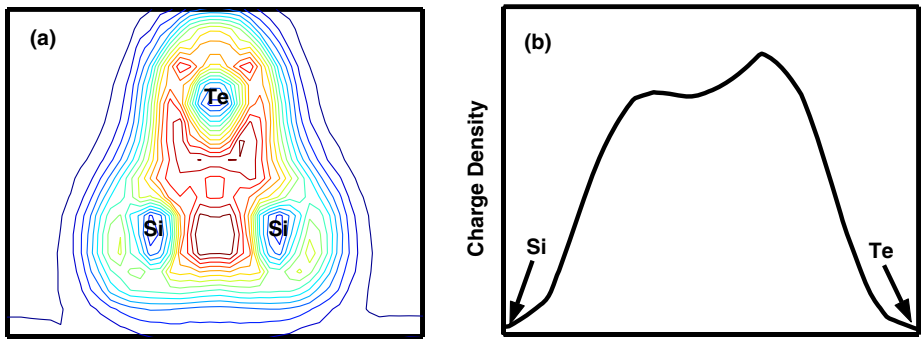

Figure 4. (a) The total charge density in a plane containing Te and edge Si atoms of the 1/6 ML covered As-passivated Si(211) surface. (b) The charge density along a line joining Te atom and its nearest Si atom (edge) when 1/6 ML Te is adsorbed on the As-passivated Si(211) surface.

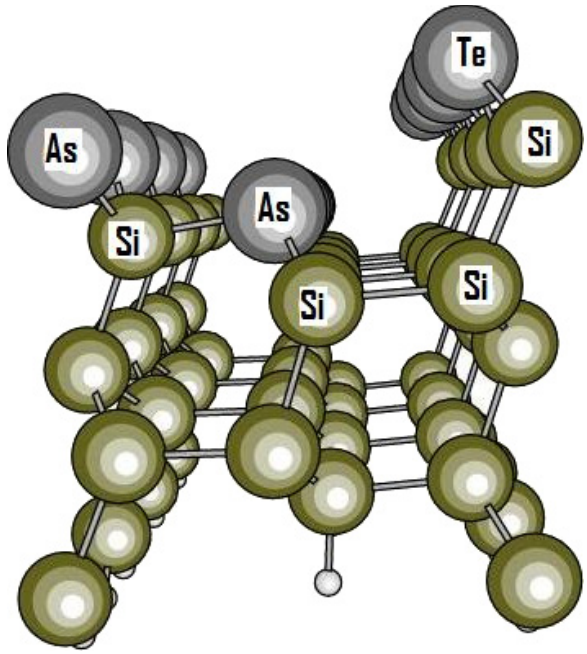

Figure 5. Stable atomic structure when 1/3 ML of Te is adsorbed on the As-passivated Si(211) surface. This clearly shows that the edge dimers are broken and hence the reconstruction of the As-passivated Si(211) surface is almost lifted.

third Te on the As-exposed Si(211) surface. This suggests that no more Te atom is allowed to bind on the 1/3 ML Te covered, As-passivated Si(211) surface and therefore, the Te coverage on the As-passivated Si(211) surface should be around 33% of one monolayer. Recent experiments [26, 27] found that the Te coverage on the As-passivated Si(211) is around 27–30% and this experimental result more or less agrees with our finding. We therefore, proceed with the 1/3 ML Te covered, As-passivated Si(211) surface for understanding the structural evolution due to the ZnTe growth on the As-exposed Si(211). Note that there was an attempt earlier [24] to understand the Te coverage on the As-passivated Si(211), however, the study was not complete.

Since, our intention is to understand the microscopic atomic structure of the ZnTe adsorbed, As-passivated Si(211) surface, we place Zn and Te atoms alternatively on the 1/3 ML covered As-passivated Si(211) surface with increasing coverage and find the most favorable adsorption sites by comparing the binding energies. At the end, we calculate the maximum energy gain of the final structure when a certain amount of ZnTe is adsorbed on the As-exposed Si(211) surface.

Now Zn atoms are adsorbed on the 1/3 ML Te covered As-passivated Si(211) surface with increasing coverage and it is found that only 1/3 ML Zn (two Zn atoms within the 1×2 supercell) binds weakly on the surface. The average binding energy per Zn atom is ∼0.2 eV and the distance between a Zn atom and its nearest Te or As atoms is ∼3 Å. When a third Zn atom is placed within the 1×2 supercell of the surface in the presence of two Zn atoms, the third Zn atom is repelled (binding energy becomes negative) and does not bind to the surface at all. Therefore, the maximum allowed Zn coverage on the 1/3 ML Te covered As-passivated Si(211) is 1/3 ML and the corresponding atomic structure is shown in figure 6.

We next consider the surface as shown in figure 6 and calculate the total energy to understand the possible adsorption of Te atoms on this surface. In this case our study shows that the possible Te coverage on the surface (shown in figure 6) is 1/3 ML with an average binding energy of ∼3.6 per Te atom. More than 1/3 ML coverage of Te on this surface is not energetically allowed (binding energy becomes negative). The most favorable atomic structure of the As-passivated Si(211) with subsequent adsorption of 1/3 ML Te, 1/3 ML Zn and then 1/3 ML Te is shown in figure 7. The atomic structure (see figure 7) very much resembles the ideal Si(211). In this configuration, the Zn–As bond lengths are ∼2.65 Å, the Zn–Te bond lengths are ∼2.5–2.6 Å, and Si–As bond lengths are ∼2.4 Å. We notice from the distribution of bond lengths that the Zn atoms which were bound weakly (see figure 6) with the surface As atoms are now bound strongly with the nearest As and Te atoms. Therefore, the presence of Te atoms insists the Zn atoms to bind strongly to the surface.

Finally, we consider the surface as shown in figure 7 and place Zn atoms within the 1×2 supercell to have an idea about the growth of ZnTe on the As-passivated Si(211) surface. There are various choices for placing Zn atoms one after another. Our detailed total energy calculations reveal that only 1/3 ML of Zn adsorption is allowed on the surface shown in

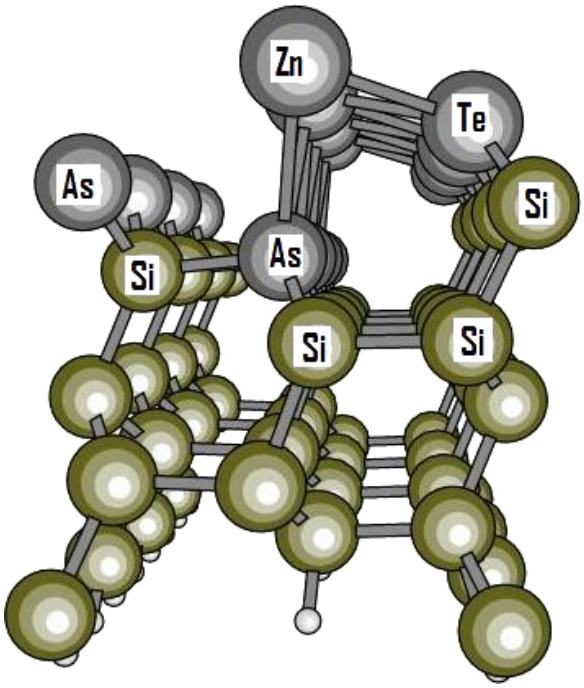

Figure 6. The atomic structure of the As-passivated Si(211) surface after the successive adsorption of 1/3 ML of Te and 1/3 ML of Zn.

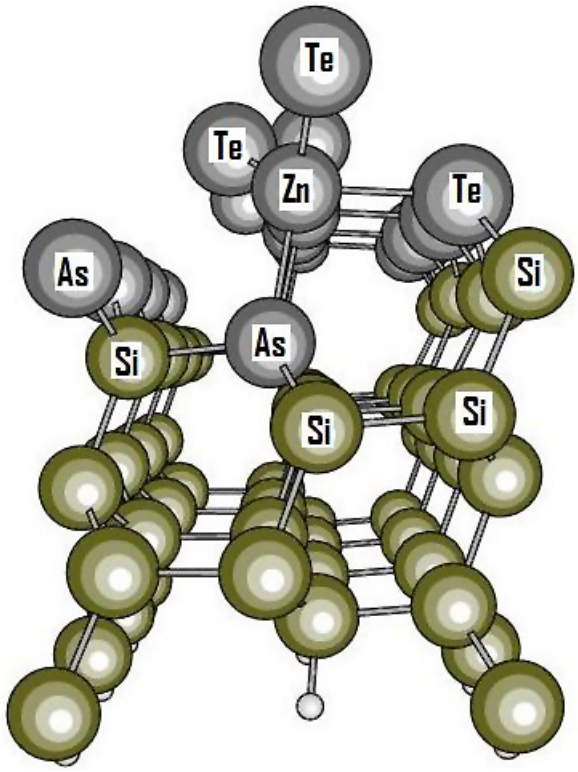

Figure 7. The atomic structure of the As-passivated Si(211) surface after the successive adsorption of 1/3 ML of Te, 1/3 ML of Zn and then 1/3 ML of Te.

figure 7 with a binding energy of 0.7 eV per Zn atom. The energetically favorable atomic structure of the As-passivated Si(211) with systematic adsorption of 1/3 ML of Te, 1/3 ML of Zn, 1/3 ML of Te and then 1/3 ML of Zn is shown in

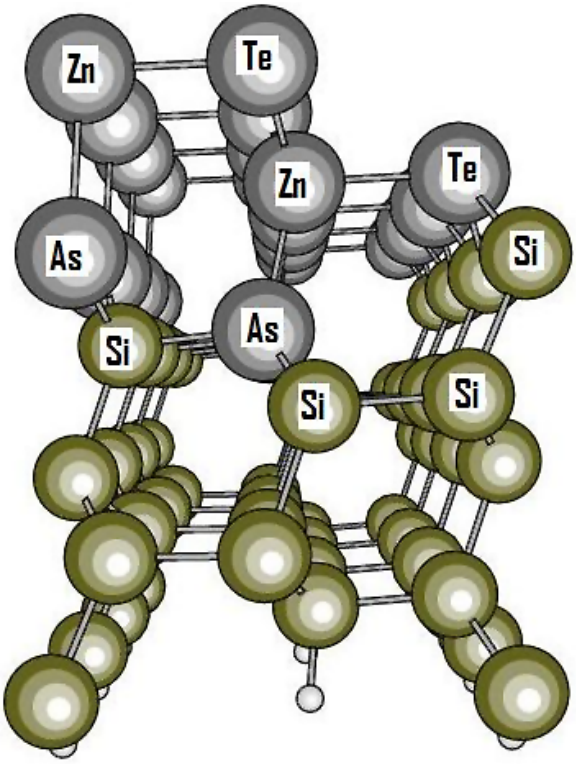

Figure 8. The atomic structure of the As-exposed Si(211) surface with subsequent adsorption of 1/3 ML Te, 1/3 ML Zn, 1/3 ML Te and then 1/3 ML Zn. The atomic structure resembles the ideal Si(211) surface structure.

figure 8. Figure 8 clearly indicates that the structure follows the ideal Si(211) structure during the initial growth of ZnTe on the As-passivated Si(211). In this structure, the bond length distributions are as follows. All the Si–As bond lengths are ∼2.4 Å. The Te atoms make a strong bond with the edge Si atoms and the corresponding Te–Si bond lengths are 2.6 Å. The Zn atoms attached to trench As atoms make a stronger bond with a bond length of 2.54 Å while the Zn atoms attached to terrace As atoms make a comparatively weaker bond with a bond length of 2.9 Å. Also note that among all the Zn–Te bonds, the nearly horizontal Zn–Te bonds (2.8 Å) are comparatively weaker with respect to other Zn–Te bonds (2.55 Å). Therefore, as a whole, we notice that after the adsorption of 2/3 ML of Te and 2/3 ML of Zn on the As-passivated Si(211), the surface structure becomes highly symmetric and resembles with the ideal Si(211). However, there are alterations of various bond lengths when compared with the ideal Si(211) and it is quite natural because of the lattice mismatch between Si and ZnTe materials. The maximum energy gain per 1×2 supercell due to the adsorption of 2/3 ML Te and 2/3 ML Zn on the As-exposed Si(211) surface is $\Delta E_{\max} = -(E_c[\text{As-exposed Si}(211) + 4\text{Te} + 4\text{Zn}] - E_c[\text{As-exposed Si}(211)]) - 4|\mu_{\text{Te}}^{\text{Bulk}}| - 4|\mu_{\text{Zn}}^{\text{Bulk}}| = -(-185.8 + 167.89) - 12.64 - 4.48)$ eV $\approx$ 0.8 eV. Note that $E_c[\text{As-exposed Si}(211) + 4\text{Te} + 4\text{Zn}] = -185.8$ eV represents the cohesive energy of 2/3 ML of Te and 2/3 ML of Zn adsorbed As-exposed Si(211) surface within the 1×2 supercell, $E_c[\text{As-exposed Si}(211)]$ represents the cohesive energy of the As-exposed Si(211) surface within the 1×2 supercell and

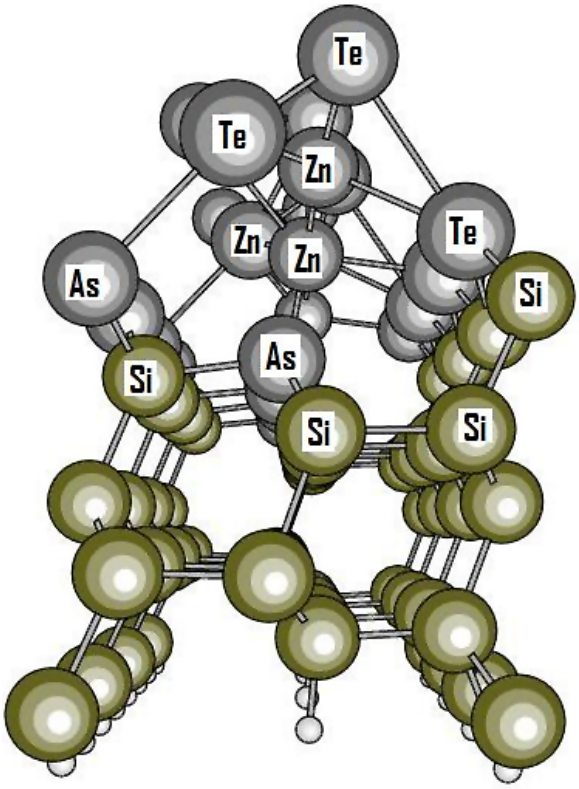

Figure 9. The atomic structure of the As-exposed Si(211) after the subsequent adsorption of 2/3 ML Te and then 2/3 ML Zn. The structure is shown within the 1×4 supercell.

$\mu_{\mathrm{Zn}}^{\mathrm{Bulk}} = 1.12$ eV is the bulk chemical potential of Zn. Finally we note, for the final structure (shown in figure 8) after the adsorption of 2/3 ML Te and 2/3 ML Zn on the As-exposed Si(211), the maximum possible energy gain per 1×2 supercell is ≈0.8 eV. This energy gain is to be compared with the maximum energy gain corresponding to other possible structures (considered in section 3.3) for determining the most favorable structure after the adsorption of ZnTe on As-exposed Si(211).

3.3. Te and Zn adsorption on As-passivated Si(211) surface: the second approach

In the first approach, we found a drastic fall in the binding energy for the Te adsorption on the As-exposed Si(211). Therefore, considering such a transition in the binding energy and the available experimental findings for Te coverage on As-passivated Si(211), we restricted the Te coverage at 1/3 ML on the As-passivated Si(211). However, here, we try to continue with the Te adsorption beyond 1/3 ML on the As-passivated Si(211) and look at the end structure and the energetics after the adsorption of 2/3 ML Te and 2/3 ML Zn. We find that 2/3 ML Te coverage is energetically allowed on the As-passivated Si(211) surface. Then we put Zn atoms on the 2/3 ML covered, As-passivated Si(211) and the total energy calculations reveal that only 2/3 ML Zn adsorption is allowed on the 2/3 ML Te covered, As-passivated Si(211) surface. The atomic structure of the As-passivated Si(211) after the subsequent adsorption of 2/3 ML Te and 2/3 ML Zn is shown in figure 9. We clearly notice that the structure is very different from the structure shown in figure 8. In fact, a cluster of ZnTe is formed on the As-passivated Si(211). In this case the maximum possible energy gain per 1×2 supercell is ≈0.5 eV. Thus, by comparing the maximum possible energy gain per 1×2 supercell, we find that the structure shown in figure 8 is more favorable than the structure shown in figure 9. We therefore, conclude that the most stable structure during the initial growth of ZnTe on the As-passivated Si(211) is the one shown in figure 8 and the structure does resemble the ideal Si(211) surface structure. We further stress the fact that the growth of ZnTe on the As-passivated Si(211) prior to the growth of CdTe and HgCdTe is desirable to minimize the growth of defects, or in other words, to have a good growth of ultimate HgCdTe on the As-passivated Si(211).

4. Conclusion

We have carried out density functional total energy calculations to understand how the atomic structure of the As-exposed Si(211) evolves during the initial growth of ZnTe on the As-exposed Si(211) surface. Our systematic consideration of all possible configurations for the adsorption of Zn and Te on the As-exposed Si(211) and a careful analysis of the energetics reveal that initial growth of ZnTe on the As-passivated Si(211) follows the ideal Si(211) structure. Therefore, it is a good idea to deposit ZnTe on the As-exposed Si(211) prior to the growth of CdTe and HgCdTe. Further work is necessary to understand the growth of CdTe on the ZnTe deposited, As-exposed Si(211) [27].

Acknowledgments

This work was partially supported by Microphysics Laboratory, Department of Physics, University of Illinois at Chicago. One of the authors, Bikash C Gupta acknowledges the partial financial support from the CSIR sponsored project, 03(1081)/06/EMR-II.

References

[1] Dabrowski J and Müssig H-J (ed) 2000 *Sillicon Surfaces and Formation of Interfaces* (Singapore: World Scientific)
[2] Venables J A (ed) 2000 *Introduction to Surface Thin Film Processes* (Cambridge: Cambridge University Press)
[3] Chadi D J 1984 *Phys. Rev.* B **29** 785
[4] Olshanetsky B Z and Mashanov V I 1981 *Surf. Sci.* **111** 414
[5] Dhar N K, Goldsman N and Wood C E C 2000 *Phys. Rev.* B **61** 8256
[6] Rujirawat S, Almeida L A, Chen Y P, Sivananthan S and Smith D J 1997 *Appl. Phys. Lett.* **71** 1810
[7] Yang B, Xin Y, Rujirawat S, Browning N D and Sivananthan S 2000 *J. Appl. Phys.* **88** 115
[8] Smith D, Tsen S-C Y, Chandrasekhar D, Crozier P A, Rujirawat S, Brill G, Chen Y P, Srorken R and Sivananthan S 2000 *Mater. Sci. Eng.* B **77** 93
[9] Rujirawat S 2000 The CdTe/Si(111): As interface *PhD Thesis* University of Illinois at Chicago, USA
[10] Baski A A and Whitman L J 1995 *Phys. Rev. Lett.* **74** 956
[11] Baski A A, Erwin S C and Whitman L J 1997 *Surf. Sci.* **392** 69

[12] Baski A A, Erwin S C and Whitman L J 1999 *Surf. Sci. Lett.* **423** L265
[13] Erwin S C, Baski A A, Whitman L J and Rudd R E 1999 *Phys. Rev. Lett.* **83** 1818
[14] Crain J N, McChesney J L, Zheng F, Gallagher M C, Snijders P C, Bissen M, Gundelach C, Erwin S C and Himpsel F J 2004 *Phys. Rev.* B **69** 125401
[15] Wright S L, Kroemer H and Inada M 1984 *J. Appl. Phys.* **55** 2916
[16] Berghaus T, Brodee A, Neddermeyer H and Tosch S 1987 *Surf. Sci.* **184** 273
[17] Wang X and Weinberg W H 1994 *Surf. Sci.* **314** 71
[18] Kaplan R 1982 *Surf. Sci.* **116** 104
[19] Sen P, Batra I P, Sivananthan S, Grein C H, Dhar N K and Ciraci S 2003 *Phys. Rev.* B **68** 045314
[20] Romano L T, Bringans R D, Zhou X and Krik W P 1995 *Phys. Rev.* B **52** 11201
[21] Fulk C *et al* 2005 private communication
[22] Brill G, Chen Y, Dhar N K and Singh R 2003 *J. Electron. Mater.* **32** 717
[23] Bringans R D 1992 *Crit. Rev. Solid State Mater. Sci.* **17** 353
[24] Gupta B C, Batra I P and Sivananthan S 2005 *Phys. Rev.* B **71** 075328
[25] Fulk C, Sporken R, Gupta B, Batra I, Zavitz D, Dumont J, Trenary M, Dhar N, Dinan J and Sivananthan S 2005 *J. Electron. Mater.* **34** 846
[26] Jaime-Vasquez M, Martinka M, Jacobs R N and Groenert M 2006 *J. Electron. Mater.* **35** 1455
[27] Dhar N K, Boyd P R, Martinka M, Dinan J H, Almeida L A and Goldsman N 2000 *J. Electron. Mater.* **29** 748
[28] Mankefors S 1999 *Surf. Sci.* **443** 99
[29] Vanderbilt D 1990 *Phys. Rev.* B **41** 7892
Kresse G and Hafner J 1994 *J. Phys.: Condens. Matter* **6** 8245
[30] Perdew J P and Wang Y 1992 *Phys. Rev.* B **46** 6671
[31] Kresse G and Hafner J 1993 *Phys. Rev.* B **47** R558
Kresse G and Furtmüller J 1996 *Phys. Rev.* B **54** 11169